

REVERSIBLE AXIAL FAN WITH BLADES CREATED OF SLIGHTLY DISTORTED PANEL PROFILES

UDC 621.634

**Božidar Bogdanović, Jasmina Bogdanović-Jovanović,
Živan Spasić, Saša Milanović**

Faculty of Mechanical Engineering, A. Medvedeva 14, Niš, Serbia

E-mail: bozidar@masfak.ni.ac.rs

Abstract. *Reversible axial fans consist of a fan runner only; they usually have runner blades, whose cylindrical cross-sections are panel-like or symmetrical lens-shaped profiles. There are also structures where runner blade's cylindrical cross-sections are slightly distorted panel profiles, but in engineering literature there is not a great deal of data about such profile cascades. Since the flow on cylindrical flow surfaces can be mapped into the flow through straight plane profile cascade, the basis for designing axial fans is given by the theory of fluid flow through straight plane profile cascades. Using the Fortran program for flow through straight plane profile cascades, developed at the Faculty of Mechanical Engineering in Niš, an analysis of the flow through profile cascades created of slightly distorted panel profile is carried out. The paper also includes the presentation of a procedure for designing this kind of profile cascades.*

Key Words: *Reversible, Axial Fan, Profiles, Profile Cascade*

1. INTRODUCTION

Low pressure reversible axial fans, designed according to scheme K (consisting of runner only), are usually composed of runner blades whose cylindrical cross-sections are panel like, or symmetrical lens-shaped profiles, as is shown in Fig.1.a and Fig.1.b for one plane developed cylindrical cross-section.

There are also structures where runner blade's cylindrical cross-sections are slightly distorted panel profiles, as is shown in Fig. 1.c, and this kind of blade profiles is the subject of this paper.

The blade shape of an axial fan is defined by more (at least five), approximately equally distant, cylindrical cross-sections.

Fig.1 also shows hub and shroud profiles, given in the profile disposition according to the top the blade height.

Reversible operation of this fan is achieved by alteration of the rotation direction of the runner.

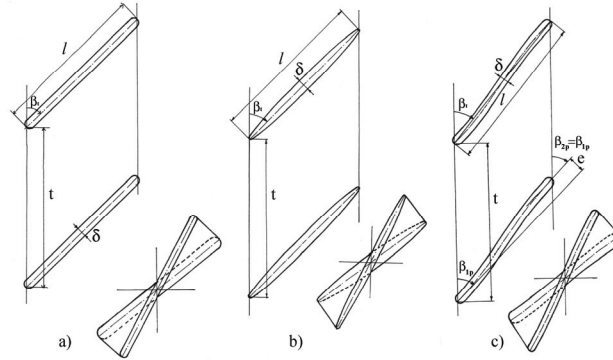


Fig. 1 Plane developed cylindrical cross-section

2. SCHEMATIZATION OF THE FLUID FLOW

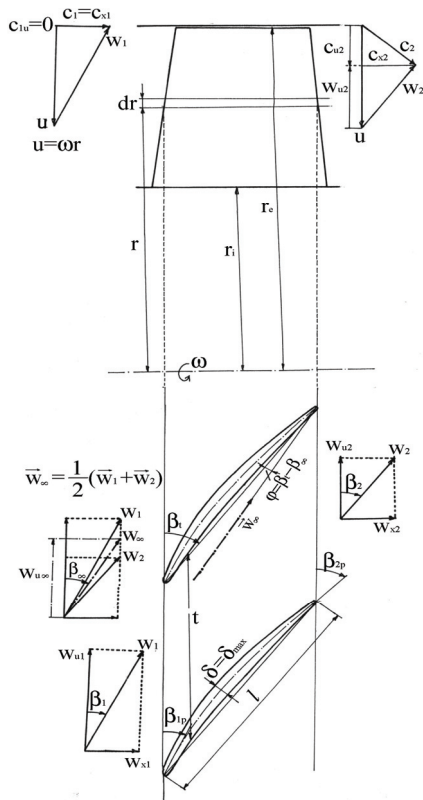


Fig. 2 Velocity triangles in front of and behind the straight plane profile cascade

With respect to the pressure changes, the air in the low pressure fan acts as an incompressible fluid ($\rho = \text{const.}$).

As in other axial turbomachinery, the designing of the axial fans has been performed according to the requirement that stream surfaces are cylindrical ($r = \text{const.}$). The space between two elementary close cylindrical stream surfaces ($r = \text{const.}$ and $r + dr = \text{const.}$ ($dr = \text{const.}$)) represents an elementary stage of the fan runner. Therefore, the fluid flow in the fan runner can be divided into a large number of elementary stages. The runner blade contour on the cylindrical stream surface ($r = \text{const.}$) creates profile cascade of the elementary stage.

Fluid flow in the turbomachinery is turbulent, defined by relatively high Reynolds number, as the characteristic value of the turbulence. In the nominal working regime of turbomachinery, when the boundary layer around blades is thin, kinematic characteristics of fluid flow (stream lines and velocity distribution) obtained by the calculation according to the model of inviscid flow corresponds well to the real kinematic characteristics of the mean turbulent flow. This is the reason to seriously take into consideration these calculations, using the inviscid flow model and these calculations play a considerable role in the design of turbomachinery, especially axial one.

According to the theory of flow of the inviscid incompressible fluid, besides necessary condition of cylindrical physical boundary surfaces of the hub ($r_1 = \text{const.}$) and the shroud ($r_e = \text{const.}$), the conditions that enable cylindrical stream surfaces in the fan runner are:

- a) To obtain an equal velocity component fields, in the axial direction, in front of (1) and behind (2) the fan runner,

$$c_{x1} = c_{x2} = \text{const.}, \text{ for absolute velocity,}$$

$$\text{and } w_{x1} = w_{x2} = \text{const.}, \text{ for relative velocity } (w_x = c_x)$$

- b) To obtain an equal head value of all elementary stages

$$Y_k(r) = u \cdot \Delta w_u = \omega \cdot r \cdot \Delta w_u(r) = \text{const.} = Y_k, \text{ for } r = \text{const.}, \quad (1)$$

where: r – radius of the cylindrical flow surface, ω – angular velocity of the fan runner, $\Delta w_u(r) = w_{u1}(r) - w_{u2}(r)$ the difference between circumferential components of relative velocities in front of (1) and behind (2) the profile cascade of the elementary fan runner stage. The positive sign is, formally, given to the components w_u which are directed opposite to the direction of the circumferential velocity (u), as is shown in the Fig. 2.

Regarding the coordinate system that rotates with the fan runner, the relative fluid flow on the cylindrical surface in the fan runner can be mapped into the flow of the straight plane profile cascade (Fig. 2). Denoting z – number of blades, the blade spacing is $t = 2\pi/z$.

According to Thomson's theorem for flow of the inviscid fluid, absolute flow in turbomachinery is vortex free ($\text{rot} \vec{c} = 0$), and since there is a relationship between absolute (\vec{c}) and relative (\vec{w}) velocity, there is also the relationship:

$$\vec{c} = \vec{w} + [\vec{\omega}, \vec{r}],$$

The relative fluid flow in the fan runner is characterized by vortex field, with angular velocity of the fluid elements (related to the fan runner)

$$\vec{\Omega} = \frac{1}{2} \text{rot} \vec{w} = -\vec{\omega},$$

where: $\vec{\omega}$ – vector of angular velocity of the fan runner ($\vec{\omega} = \pm \omega \cdot \vec{x}^0$, \vec{x}^0 - unit vector in the direction of fan axis).

The vortex lines of the relative flow in the fan runner are lines parallel to the fan axis, and therefore they lie on cylindrical surfaces.

Hence $\text{rot} \vec{w} = -2\vec{\omega}$ has no component perpendicular to the cylindrical flow surface ($r = \text{const.}$), the following conclusions can be made:

- 1) Circulation of relative velocities around a closed contour on the flow surface is equal to zero, in the cases when the closed contour does not contain blade profiles (according to Cauchy theorem).
- 2) Differential equations for obtaining relative velocities and streamlines on cylindrical flow surfaces in rotational axial fan runner are of the same shape as equations for obtaining absolute velocities and their streamlines on cylindrical flow surfaces in stationary blade stators.

The above-specified conclusions are also valid for the flows mapped into the plane (for a relative flow through the straight plane profile cascade, that the relative flow on cylindrical flow surface in the rotational runner is mapped into, respectively for the absolute flow through the straight plane profile cascade, that the absolute flow in the stationary blade stator is mapped into). This is the reason why the results of the calculations of the fluid flow through the straight plane profile cascade, obtained for vortex free absolute flow ($\text{rot}\bar{c} = 0$) of the inviscid fluid, can be used also in practice for relative vortex flows through straight plane profile cascades.

The vortex lines of the flows mapped into the plane lie in the plane of the straight plane profile cascade (lines perpendicular to the plane cascade axis) and they do not affect kinematic characteristics of the flow mapped into the plane.

In Fig. \bar{w}_1 and \bar{w}_2 denote flow velocities in front of and behind the profile cascade (theoretically, velocities in front of and behind the profile cascade), whereas

$$\bar{w}_\infty = \frac{1}{2}(\bar{w}_1 + \bar{w}_2),$$

is called the mean velocity in infinity.

3. THEORETICAL RESULTS OF FLOW CALCULATION THROUGH THE STRAIGHT PLANE PROFILE CASCADE

Denoting with Γ_p velocity circulation around the profile contour,

$$\Gamma_p = \int_{L_p} \mathbf{v}(s) \cdot d\mathbf{s}, \quad (2)$$

according to the theory of vortex-free fluid flow of the incompressible inviscid fluid through straight plane profile cascade, it is easy to show that there is a relationship between angles of flow directions behind (β_2) and in front of (β_1) profile cascade:

$$\text{ctg}\beta_2 = \text{ctg}\beta_1 - \frac{\Gamma_p}{v_{x1} \cdot t}, \quad (3)$$

and that the lift coefficient of the profile can be obtain by an equation:

$$\xi_y = \frac{2\Gamma_p}{v_\infty \cdot l}, \quad (4)$$

where: t – blade spacing (space between blade profiles), l – chord length (longitude of the line connecting leading and trailing edges of the profile camber line), v_{x1} ($v_{x1} = v_{x2}$) – magnitude of the effluent velocity component in front of and behind profile cascade, v_∞ – magnitude of the mean velocity in infinity, $\mathbf{v}(s)$ – velocity distributions around the profile contour.

In equations (2)-(4) flow velocities are denoted with v , since the calculation results of the flow through straight plane profile cascade can be applied to the flow mapped into the plane of cylindrical flow surface ($r = \text{const.}$) in the stationary blade stator ($v = c$), as well as to the relative flow ($v = w$) mapped into the plane of cylindrical flow surface in the rotational runner.

According to equations (2), (3) and (4), and with respect to theoretically determined $v(s)$ and β_2 , where β_1 varies, Weinig has obtained a diagram for the deflection coefficient of the straight plane cascade of the thin profiles and circular arc camber line of the profiles (Fig.5). For the flow through cascades created of thin panel profiles the diagram is also obtained of the profile lift coefficient in cascade and lonely profile lift coefficient ratio (Fig.5).

The deflection coefficient of the cascade created of thin profiles and circular arc camber line of the profiles is defined by relation $\sigma_R = \Delta\beta^+/\theta$, where $\theta = \beta_{p2} - \beta_{p1}$ profile camber angle (β_{p1} and β_{p2} - profile leading and trailing edge angle), $\Delta\beta^+ = \beta_2^+ - \beta_1^+$ is angular deflection due to profile cascade. Superscript + denotes a shock-free flow, when fluid flows to the profiles in direction which is tangential to the profile camber line. The deflection coefficient of the cascade created of thin profiles and circular camber line of the profiles, as is shown in Fig.3, depends on relative blade spacing $\bar{t} = t/l$ and angle of average flow deflection $\bar{\beta} = 0,5(\beta_1 + \beta_2)$.

Weinig's diagram is an important element in axial pump impellers and fan runners designing, where blades are formed from circular arc camber line profiles. It is an interesting fact that this diagram gives very good results also for profiles camber line different from circular arc.

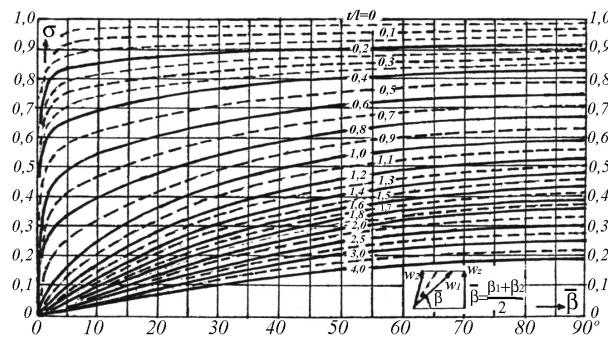


Fig. 3 Weinig's diagram $\sigma_R = \Delta\beta^+/\theta$

Lift coefficient of panel profile in cascade made of panel profiles can be calculated by using a formula:

$$\xi_y = K_0 \cdot 2\pi \sin \delta, \quad (5)$$

where: $\varphi = \beta_\infty - \beta_t$ incidence of mean velocity in infinity (Fig.4), K_0 - coefficient which depends on relative blade spacing $\bar{t} = t/l$ and chord angle β_t . Fig.5 shows Weinig's diagram, theoretically obtained, for $K_0 = K_0(\bar{t}, \beta_t)$.

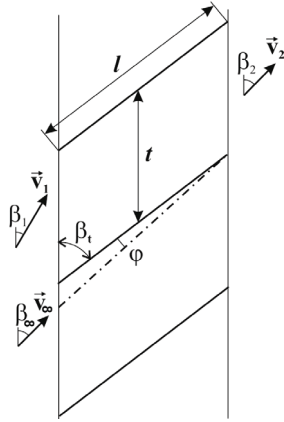


Fig. 4 Shock-free entry to the thin panel profile cascade

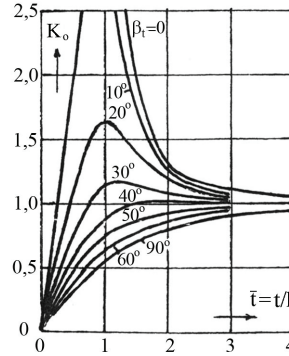


Fig. 5 Weinig's diagram $K_0(\bar{t}, \beta_1)$

The Department of Hydroenergetics of Mechanical Faculty in Niš has developed a computer software for calculation of vortex free inviscid fluid flows through straight plane profile cascades, in shock-free entry [2]. This task is solved by using the method of conformal mapping. The flow around a profile contour is mapped, in auxiliary plane $\zeta = \xi + i\eta$, to the flow around a contour belt $\zeta = \xi + i\pi/2$ and $\zeta = \xi - i\pi/2$, and the flow far away in front of and behind the profile cascade is mapped into singular points $\zeta = \xi = -k$ and $\zeta = \xi = k$, as is shown in Fig.6. Details of the mapping principles are discussed in papers [3] and [4], and further on in the text some basic mapping characteristics are presented.

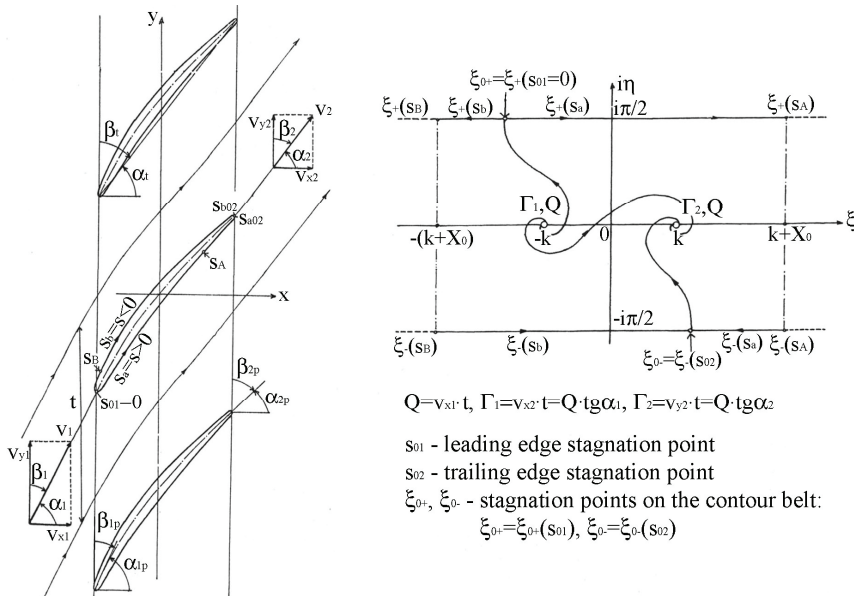


Fig. 6 Flow mapping

For the sake of simplicity, as is shown in Fig.6, the coordinates of the contour belt are denoted ξ_+ and ξ_- . Measured from the contour leading edge stagnation point of the profile ($s_{01} = 0$), the coordinates of the profile sides contours are denoted in Fig.6 as s_a and s_b . Therefore, the trailing edge point, depending of the approaching side, has two coordinates: s_{a02} and s_{b02} . Accepting Δs as a negligible small longitude of the profile contour, which can be considered in calculations as a point in the profile contour, two points on the profile contour, s_A and s_B in Fig.6, are mapped, using an infinite extension, to the contour belt $\xi_{\pm} \geq k + x_0$ and $\xi_{\pm} \leq -(k + x_0)$. Dimension k which defines positions of the singular points in the belt ($\xi = \pm k$) is a parameter of the mapping domain that depends only on the geometrical parameters of the profile cascade.

The points where the camber line touches round front and back profile line defines the leading and the trailing edges. In the calculation of the flow through a profile cascade, the trailing edge is fixed on the profile output (Zukovski-Capljigin postulate), whereas the leading edge is in the input profile point only in the case of shock-free entry.

In the program for shock-free flow calculation, all longitudinal parameters of the profile cascade are derived on the dimensionless form, according to unit camber line ($l_{sk} = 1$). Angular parameters importing to program (α_{p1} , α_{p2} and α_t), as well as calculated flow angles in front of and behind the profile cascade (α_1 and α_2) that are being calculated, are defined according to the direction perpendicular to the profile cascade axis. There are relationships between those angles and the angles measured according to the direction of the cascade axis (β):

$$\alpha_{p1} = 90^\circ - \beta_{p1}, \quad \alpha_{p2} = 90^\circ - \beta_{p2}, \quad \alpha_t = 90^\circ - \beta_t, \quad \alpha_1 = 90^\circ - \beta_1, \quad \alpha_2 = 90^\circ - \beta_2.$$

In this program $s_a = s > 0$ ($v(s_a) = v(s)$), and coordinate s_b and velocity $v(s_b)$ are formally given negative signs: $s_b = s < 0$ and $v < 0$, for $s < 0$.

The imported geometrical parameters of the profile cascade are: angles α_{p1} (ALF1P), α_{p2} (ALF2P), α_t (ALFT) and dimensionless parameters: blade spacing t (TL) and coordinates of the trailing edge stagnation points $s_{02} > 0$ (SOA) and $s_{02} < 0$ (SOB). Subroutine ALFA(S) gives us functional dependency of the angle of the profile cord line around a profile contour ($\alpha(s)$), for $s=0$ on the leading edge.

If $\alpha_0(s)$ denotes $\alpha(s)$ for $\alpha_t=0$, any different angle α_t gives us relation: $\alpha(s) = \alpha_t + \alpha_0(s)$, therefore by changing α_t the subroutine ALFA(S) is adapted for different angles.

The calculation results are printed obtained values $k(K)$, $x_0(X0)$, ξ_{0+} (KSI1), ξ_{0-} (KSI2), $s_A > 0$, $s_B < 0$, α_1 (ALFA1), α_2 (ALFA2), and the table of correspondence $s - \xi_{\pm}$ (S-OP), for $s > 0$ and $s - \xi_{\pm}$ (S-ON), for $s < 0$, and velocity distribution around a profile contour $s - \bar{v}(s)$ for $s > 0$ and $s < 0$, where $\bar{v}(s) = v(s)/v_{x1}$ is dimensionless velocity. In Table $s - \bar{v}(s)$ there is a third column $\bar{\Gamma}(s)$:

$$\bar{\Gamma}(s) = \int_0^s \bar{v}(s) \cdot ds.$$

Velocity circulation around a profile contour is: $\Gamma_p = v_{x1}(\bar{\Gamma}(s_{02} < 0) - \bar{\Gamma}(s_{02} > 0))$.

Denoting α_1^+ ($\beta_1^+ = 90^\circ - \alpha_1^+$), α_2^+ ($\beta_2^+ = 90^\circ - \alpha_2^+$) and $\bar{v}^+(s)$ as previously obtained results for shock-free flow, according to parameter k and correspondence $\xi_{\pm}(s)$, changing the angle α_1 ($\alpha_1 = 90^\circ - \beta_1$) the following relation is obtained:

$$\alpha_2 = \operatorname{arctg} \frac{\operatorname{tg} \alpha_1 \operatorname{ch}(\xi_{0-} - k) + \operatorname{sh} 2k}{\operatorname{ch}(\xi_{0-} + k)}, \text{ and} \quad (6)$$

$$\bar{v}(s) = \frac{\pm [\operatorname{tg} \alpha_1 \operatorname{ch}(\xi_{\pm}(s) - k) - \operatorname{tg} \alpha_2 \operatorname{ch}(\xi_{\pm}(s) + k)]}{\pm [\operatorname{tg} \alpha_1^+ \operatorname{ch}(\xi_{\pm}(s) - k) - \operatorname{tg} \alpha_2^+ \operatorname{ch}(\xi_{\pm}(s) + k)]} \bar{v}^+(s), \quad (7)$$

whereas leading edge point (s_{01}) is mapped into

$$\xi_{0+} = k + \ln \frac{\operatorname{sh}(-1 + \sqrt{1+A})}{B}, \quad (8)$$

where: $A = \frac{\operatorname{ctg} \alpha_1 \cdot \operatorname{ctg} \alpha_2}{\operatorname{th} 2k \cdot \operatorname{sh} 2k} - \frac{\operatorname{tg}^2 \alpha_1 + \operatorname{tg}^2 \alpha_2}{\operatorname{sh}^2 2k}$ and $B = e^{2k} \operatorname{tg} \alpha_2 - \operatorname{tg} \alpha_1$.

Sign +, in formula (7), corresponds to $\xi_+(s)$, and sign – corresponds to $\xi_-(s)$.

Since there is relation $\beta = 90^\circ - \alpha$, according to equation (3), there is a relation:

$$\Gamma_p = v_{x1} t (\operatorname{tg} \alpha_1 - \operatorname{tg} \alpha_2), \quad (9)$$

thus, for obtaining velocity circulation around a profile contour (equation (4)) and for obtaining the lift coefficient of the profile it is sufficient to determine α_2 for given α_1 (equation (5)). Equation (4) becomes

$$\xi_y = 2\bar{t} (\operatorname{tg} \alpha_1 - \operatorname{tg} \alpha_2) \cos \alpha_\infty, \quad (10)$$

where: $\bar{t} = t/l$ is relative blade spacing and α_∞ inclination angle toward axis x of the vector $\bar{v}_\infty = 0,5(\bar{v}_1 + \bar{v}_2)$ is

$$\alpha_\infty = \operatorname{arctg}[0,5(\operatorname{tg} \alpha_1 + \operatorname{tg} \alpha_2)]. \quad (11)$$

The non-productive flow through the profile cascade is one where the velocity circulation is equal to zero ($\Gamma_p = 0$), therefore the profile cascade does not produce flow deflection ($\alpha_1 = \alpha_2$, i.e. $\beta_1 = \beta_2$), and the lift force is equal to zero ($\xi_y = 0$). In this case $\alpha_\infty = \alpha_1 = \alpha_2$ ($\beta_\infty = \beta_1 = \beta_2$) and $v_\infty = v_1 = v_2$.

The non-productive flow through cascade created of panel like profiles, or symmetrical lens shaped profiles, where δ is blade thickness (Fig.1.a and Fig.1.b), develops in shock-free flows ($\alpha_1 = \alpha_1^+$), whereby $\alpha_1^+ > \alpha_1$ for the cascades where $\alpha_t > 0$ (for $\alpha_t = 0$, $\alpha_1^+ = 0$). Therefore, for the non-productive flow ($\xi_y = 0$, $\alpha_2^+ = \alpha_1^+ = \alpha_\infty$, $v_1^+ = v_2^+ = v_\infty$) through cascade of panel profiles or symmetrical lens shaped profiles with thickness δ there is an adequate incidence angle $\varphi^+ = \alpha_\infty^+ - \alpha_t = \alpha_1^+ - \alpha_t > 0$, which can be easily obtained by the computer program. This kind of the profile cascade induces flow deflection, which corresponds to fan runner, with incidence angle $\varphi > \varphi^+$, i.e. $\alpha_1 > \alpha_1^+$ ($\beta_1 < \beta_1^+$).

For the cascade created of panel like profiles, or symmetrical lens shaped profiles ($\alpha_t > 45^\circ$, $\bar{t} = 0$, $\bar{\delta} = 0,08$), shown in Fig.7.a and Fig.7.b, it is obtained due to calculation:

- for cascade created of panel profiles: $\alpha_1^+ = 45^\circ$ ($\varphi^+ = 3,1^\circ$), $k=1,846$, $\xi_{0-} = 1,790$,
- for cascade created of lens shaped profiles: $\alpha_1^+ = 47,4^\circ$ ($\varphi^+ = 2,4^\circ$), $k=1,873$, $\xi_{0-} = 1,846$.

Since mapping parameters k and ξ_{0-} are constant for the mapped cascade, using equations (5), (11) and (10) it can be calculated magnitudes of lift coefficients for different angles of attack (α_1), i.e. for different incidences $\varphi = \alpha_{\infty} - \alpha_t$. Fig.7.c gives diagram $\xi_y(\varphi)$ for the profile cascades shown in Fig.7.a and Fig.7.b. For simplicity, Fig.7 shows diagram $\xi_y(\varphi)$ for very thin panel profiles ($\delta \rightarrow 0$), where $\alpha_t = 45^\circ$ ($\beta_t = 45^\circ$) and $\bar{t} = 1$ ($K_0 = 0,818$, $\xi_y = 5,14 \cdot \sin\varphi$). The difference between coefficients ξ_y for profiles with relative thickness $\bar{\delta} = 0,08$ and very thin profiles is approximately equal to coefficient $\xi_y(\varphi = \varphi^+)$ for very thin profiles.

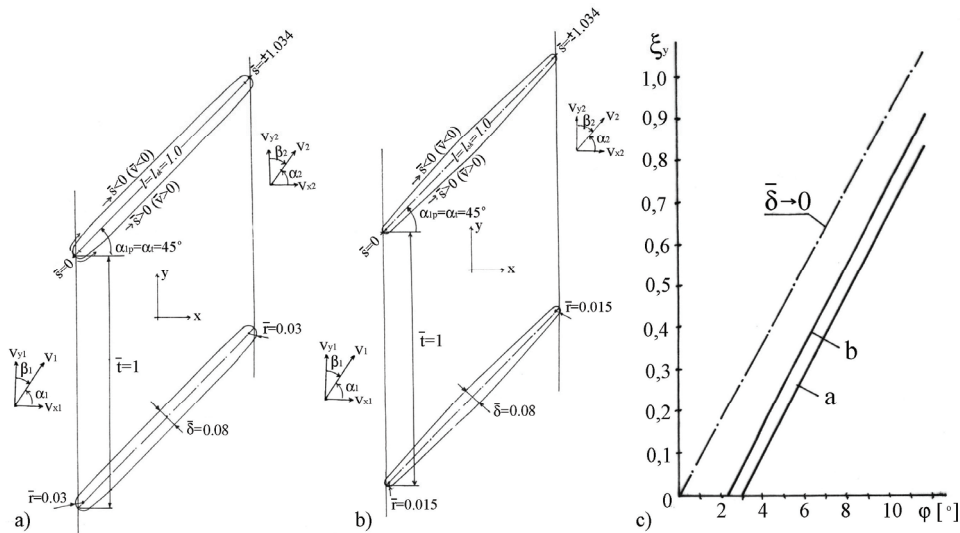


Fig. 7 Example of calculation $\xi_y(\varphi)$

Profiles shown in Fig.1.b are, in the middle, slightly distorted panel profiles, and they have the same deflection angles in front of and behind the profile ($\alpha_{2p} = \alpha_{1p}$). Backward eccentric dislocation of the profile tail related to profile forehead (e) is a longitudinal coordinate of the panel profile distortion. Stagger angle differs from the deflection angle in front of and behind the profile cascade ($\alpha_t > \alpha_{1p}(= \alpha_{2p})$, i.e. $\beta_t < \beta_{1p}(= \beta_{2p})$).

Fig.8 shows two plane profile cascades made of slightly distorted panel profiles, where $\bar{e} = 0,05$ and $\bar{e} = 0,10$.

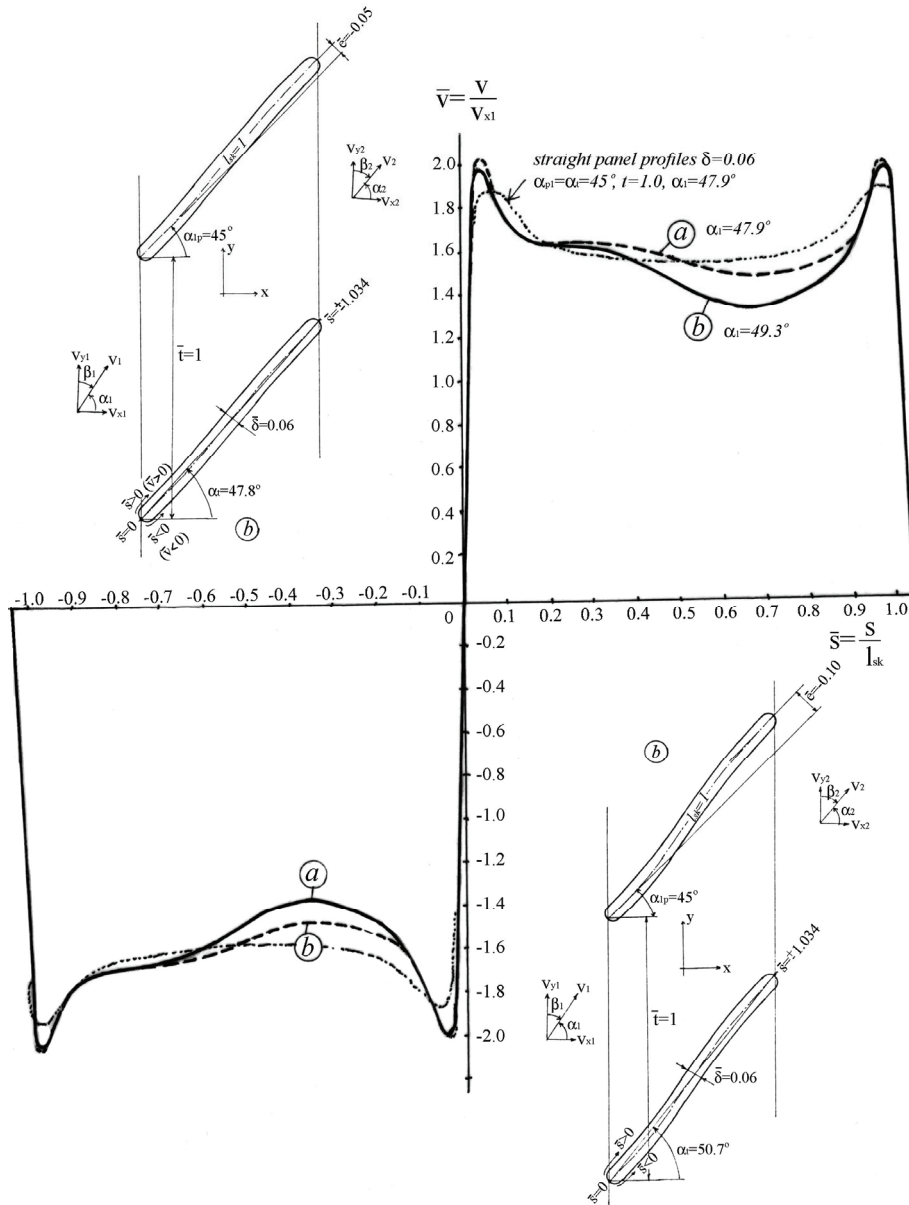


Fig. 8 Velocity distribution around the profile

All the longitudinal parameters are derived to dimensionless form, according to camber line $l_{sk} = 1$. Profile thickness is $\bar{\delta} = 0,06$, and blade spacing is $\bar{t} = 1$. Deflection angles in front of and behind the profile cascades are equal $\alpha_{2p} = \alpha_{1p} = 45^\circ$. In Fig.8.a $\bar{e} = 0,05$, $\alpha_t = 47,8^\circ$ ($\beta_t = 42,2^\circ$), and in Fig.8.b $\bar{e} = 0,10$, $\alpha_t = 50,7^\circ$ ($\beta_t = 39,3^\circ$).

In Fig.8, besides geometrical parameters, there is dimensionless velocity distribution on the profile contour ($\bar{v}(s) = v(s)/v_{1x}$), obtained by shock-free flow calculation (for unproductive fluid flow: $\alpha_2^+ = \alpha_1^+$, $\alpha_\infty^+ = \alpha_1^+$, $\xi_y = 0$). For profile cascade a), $\bar{e} = 0,05$, $\alpha_1^+ = 47,5^\circ$ ($\beta_1^+ = 42,5^\circ$), therefore $\varphi = \alpha_\infty - \alpha_t (= \beta_\infty - \beta_t)$, for unproductive flow $\varphi^+ = -0,3^\circ$, and for profile cascade b) $\bar{e} = 0,10$, $\alpha_1^+ = 49,3^\circ$ ($\beta_1^+ = 40,7^\circ$) and $\varphi^+ = -1,4^\circ$. Mapping parameters k and ξ_0 . (in equation (6)) have values: a) $k=1,748$, $\xi_0=1,729$, and b) $k=1,866$, $\xi_0=1,773$.

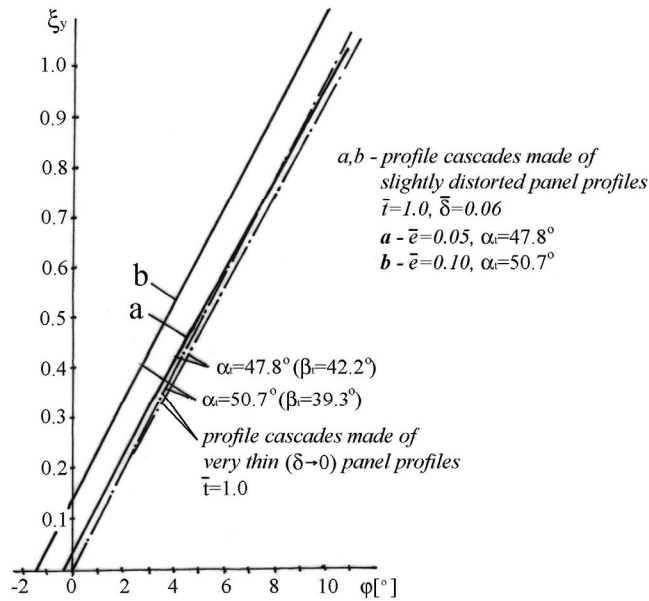


Fig. 9 Lift coefficient $\xi_y(\varphi)$

According to calculated lift coefficients, for the different angles of attack ((6), (10) and (11)), there are in Fig.9 interpolated diagrams $\xi_y(\varphi)$ for profile cascades shown in Fig.8. For the purpose of comparison, there is also graph $\xi_y(\varphi)$ for very thin panel profiles ($\bar{\delta} \rightarrow 0$), where $\bar{t} = 1$, $\alpha_t = 47,8^\circ$ and $\alpha_t = 50,7^\circ$.

For the same angle of attack, coefficients ξ_y for thin plane panel profiles $\bar{\delta}$ are less than one for very thin profiles ($\bar{\delta} \rightarrow 0$), thus, according to diagram in Fig.9, it can be concluded that the profile cascades made of slightly distorted panel profiles produce larger lift force than corresponding ($\bar{\delta} = \text{const.}$, $\bar{t} = \text{const.}$ and $\alpha_t = \text{const.}$) profile cascade made of plane panel profiles.

Like the cascades made of lance shaped or plane panel profiles, the profile cascades made of slightly distorted panel profiles can produce flow deflection only for shock flow situation. The shock flow generates conditions for the flow separation from the suction side of the profile ($s < 0$, $v(s) < 0$). Accelerated flow around the suction side of the slightly distorted panel profiles in shock flow condition indicates flow separation of the fluid flow with larger angles of attack, related to plane panel profiles.

4. THE CALCULATION OF ELEMENTARY STAGES OF THE FAN RUNNER

For the known calculated (nominal) fan working regime, the flow parameters on the axisymmetrical cylindrical flow surfaces ($r = \text{const.}$) of the elementary stages of the fan runner

$$\beta_1(r), w_1(r), \beta_2(r), w_2(r), \beta_\infty(r), w_\infty(r) \text{ and}$$

$$\Delta w_u(r) = w_{u1}(r) - w_{u2}(r), \text{ i.e. } \Delta\beta(r) = \beta_2(r) - \beta_1(r),$$

it is required to define the stagger angle (β_t) and the chord line (l) of the plane profile cascades.

For solving this task the lift force method is used. Between lift coefficient ξ_y and velocity flow deflection Δw_u of the profile cascade there is a relation:

$$\xi_y \frac{l}{t} = 2 \frac{\Delta w_u}{w_\infty}. \quad (12)$$

The camber line of plane panel and symmetrical lens shaped profiles is also the chord line for the plane panel and lance shaped profiles.

It is experimentally determined [1] that the theoretically obtained Weing's diagram for the deflection coefficient of thin circular arc camber line profiles (Fig.3) and diagram of lift coefficients in thin panel profile cascades (Fig.4) yield good practical results in cases when

$$\text{Re} = \frac{w_\infty l}{\nu} \geq 3 \cdot 10^5, \text{ i.e. } l \geq \frac{3 \cdot 10^5 \nu}{w_\infty}, \quad (13)$$

where: Re – Reynolds number, ν – coefficient of kinematic viscosity of the air ($\nu = 1,5 \cdot 10^{-5} \text{ m}^2/\text{s}$, for the air pressure 101,3 kPa and temperature 20°C).

Determined by experiment the maximum lift force and drag force ratio in plane symmetric profile cascade, Zweifel has obtained a formula for defining an optimal relative blade spacing [1]:

$$\bar{t}_{\text{opt}} = (0,4 \div 0,45) \frac{w_2^2}{w_\infty \Delta w_u}. \quad (14)$$

Formula (14) applies to the cascades made of unsymmetrical profiles.

If z is number of runner blades, blade spacing of cylindrical surface with radius r is $t = 2\pi r/z$, which leads to one more condition for determining chord line, i.e. number of blades

$$l = \frac{2\pi r}{z \cdot \bar{t}_{\text{opt}}}, \text{ i.e. } z = \frac{2\pi r}{\bar{t}_{\text{opt}} \cdot l}, \quad (15)$$

where \bar{t}_{opt} is calculated by formula (14).

After determining of chord line (t) and camber line (l), using equation (12), we can calculate lift coefficient (ξ_y), and, after, using formula (6) and diagram $K_o(t/l, \beta_t)$ (Fig.5) we can calculate incidence angle (φ) and stagger angle (β_t) of the very thin panel profiles:

$$\varphi = \arcsin \frac{\xi}{2\pi K_0}, \quad \beta_t = \beta_\infty + \varphi. \quad (16)$$

Whereby coefficient K_0 depends of angle β_t , the determination of those parameters is obtained by iterative procedure, where initial approximation is $\beta_t \approx \beta_\infty + 5^\circ$.

Angle β_t obtained by equation (16) is denoted as $\beta_t^{(1)}$, and for the real panel profile cascade, lens shaped or slightly distorted panel profile cascades it is an initial approximation angle.

For the profile cascades made of panel or lens shaped profiles, according to profile thickness (δ), stagger angle β_t is larger than $\beta_t^{(1)}$,

$$\beta_t = \beta_t^{(1)} + \varphi^+. \quad (17)$$

denoting, as is shown in chapter 3, φ^+ - incidence angle for the unproductive fluid flow through the profile cascade, where profile thickness is δ and stagger angle $\beta_t = \beta_t^{(1)}$.

As has been explained in the Section 3, the lift coefficient of a slightly distorted panel profile cascade can be larger than the lift coefficient of very thin panel profile cascade, lined at the same stagger angle, thus β_t can be smaller than $\beta_t^{(1)}$. The correction of angle β_t performs in this case using equation (17), therewith the incidence angle of unproductive flow through the slightly distorted panel profile cascade with an angle $\beta_t = \beta_t^{(1)}$ can also have a negative sign ($\varphi^+ < 0$).

CONCLUSION

According to the given theoretical solution of the flow through straight plane profile cascades made of: a) plane panel profiles, b) symmetrical lens shaped profiles and c) slightly distorted panel profiles, it can be concluded that the profile cascade c) makes the largest lift force and therefore produces the largest flow deflection, under the same conditions of relative blade spacing ($\bar{t} = \text{const.}$), stagger angle ($\beta_t = \text{const.}$) and relative thickness ($\bar{\delta} = \text{const.}$).

Using the computer program, previously presented, for shock-free entry flows, it is easy to obtain stagger angles for all three different profile cascades considered in this paper.

REFERENCES

1. Obradović N., Turbokompresori, Tehnička knjiga, Beograd, 1974.
2. Milanović S., "Calculation of the spatial fluid flow through axial turbomachinery as a complex of two two-dimensional fluid flows", master thesis, Faculty of Mechanical Engineering in Nis, 1996.
3. Bogdanović B., "Calculation of potential flow through straight plane hydrofoil cascades using a method of conformal mapping", monograph, Faculty of Mechanical Engineering in Nis, 1999.
4. Bogdanović B., Milanović S.: "Solution of the direct problem in theory of flow through straight plane profile cascade by using conformal mapping into band $-\pi/2 \leq \text{Im}Z \leq \pi/2$ ", Facta Universitatis, Series mechanical engineering, (809 ÷ 816), Vol. 1, N° 7, 2000.

**REVERZIBILNI AKSIJALNI VENTILATOR
SA LOPATICAMA FORMIRANIM OD BLAGO
ZAKRIVLJENIH PLOČASTIH PROFILA**

**Božidar Bogdanović, Jasmina Bogdanović-Jovanović,
Živan Spasić, Saša Milanović,**

Reverzibilni aksijalni ventilatori konstruisani tako da imaju samo jedno ventilatorsko kolo, najčešće imaju lopatice čiji su cilindrični preseći pločasti ili simetrični sočivasti profili. Postoje konstrukcije i sa lopaticama čiji su cilindrični preseći blago izvijeni pločasti profili, o kojima se u stručnoj literaturi praktično i ne govori.

Kako se strujanje na cilindričnim strujnim površinama može preslikati na strujanje kroz prave ravanske rešetke profila, osnovu, pri projektovanju aksijalnih ventilatora, daje teorija strujanja kroz prave ravanske rešetke profila. Koristeći, na Mašinskom fakultetu u Nišu, razvijeni program za proračun strujanja kroz prave profilne rešetke, izvršena je analiza strujanja kroz rešetke sa blago izvijenim pločastim profilima. U radu je izložen i postupak projektovanja rešetki sa blago izvijenim profilima.

Ključne reči: *reverzibilni, aksijalni ventilatori, profili, rešetke profila.*